VNU Journal of Science: Mathematics - Physics

Journal homepage: https://js.vnu.edu.vn/MaP

Original Article

The Contribution of Photon, Z Boson, Higgs, Radion and Unparticle to the Processes $e^+e^- \to e^+e^-$ in Randall-Sundrum Model

Dao Thi Le Thuy*, Le Mai Dung

Hanoi National University of Education, 136 Xuan Thuy, Cau Giay, Hanoi, Vietnam

Received 04 August 2023
Revised 03 November 2020; Accepted 18 March 2024

Abstract: The fundamentally well-known process of Bhabha $e^+e^- \to e^+e^-$ is studied from the theoretical view of unparticle physics in the prominent Randall-Sundrum model. The cross-sections independently for photon (γ), Z boson (Z), vector unparticle (U^μ), Higgs (h), radion (ϕ), and scalar unparticle (U) exchange are calculated and evaluated. Numerical calculations showed that the contribution of unparticle exchange dominates in very high energy regions. While the standard model exchanges as γ and Z are predominant in the lower energy region, h and ϕ contribution is very small in comparison with the other exchanges. The results are plotted in the energy ranges available in the present designs of accelerators and near future energy upgrades of the International Linear Collider (ILC) and The Compact Linear Collider (CLIC).

Keywords: Bhabha scattering, unparticle physics, e^+e^- collisions, ILC collider, Randall-Sundrum model.

1. Introduction

It is notable that one of the flaws in the most triumphant physical theory ever built - the Standard Model (SM) is a large hierarchy between the Planck scale and the weak scale. Afterward, a considerable number of theories were proposed with a view to solving this hierarchy problem. All the models with extra dimensions assume the world is (4+n)+1-dimensional, where the extra n space-like dimensions are compactified with a smaller radius than the present experimental probe. In the following parts, this article will concentrate on the model suggested by Randall and Sundrum (RS model) [1]. RS model

* Corresponding author.
E-mail address: thuydtl@hnue.edu.vn

https//doi.org/10.25073/2588-1124/vnumap.4867

assumes the universe is five-dimensional. RS model is not similar to ADD model [2] since a large compactification radius for an extra compactified space-like dimension is unnecessary. The radius of compactification is of the order of Planck length and is also a dynamical observable. This radius relates to the vacuum expectation value of the dilaton field appearing as a result of the compactification of 5-dimensional theory to 4 dimensions. Radion field is generated as a quantum fluctuation of the modulus of the fifth dimension. Goldberger and Wise [3, 4] proved that a scalar field propagating in the background geometry – the five-dimensional anti-de Sitter spacetime as seen in Eq. (1), can give rise to a potential that stabilizes the modulus L. The background metric of the RS1 model is as follows

$$ds^2 = e^{-2\sigma(y)}\eta_{\mu\nu}dx^\mu dx^\nu - b_0^2 dy^2 \tag{1}$$

where $\sigma(y) = m_0 b_0[y(2\theta(y)-1) - 2(y-1/2)\theta(y-1/2)]$, b_0 is a constant not determined by the five-dimensional action. Gravitational fluctuations around the metric will be defined through the following replacements

$$\eta_{\mu\nu} \to \eta_{\mu\nu} + \varepsilon h_{\mu\nu}(x,y); \quad b_0 \to b_0 + b(x) \tag{2}$$

Radion mass in the stabilized RS model is lighter than that of the Kaluza-Klein modes of all fields as graviton [3-5]. Hence, radion might be considered the first state, which is specific to the model. In the origin of the RS model, the bare parameters are defined for values by the Planck scale. The applicable value for the size of the extra dimension is adjusted by $kr_c\pi \approx 35$ (r_C is the compactification radius and k is the bulk curvature). Subsequently, the weak and gravity scales are generated naturally. The mixing of gravity and scalar has the following form

$$S_\xi = -\xi\int d^4x\sqrt{g_{vis}}R(g_{vis})\hat{H}^\dagger\hat{H} \tag{3}$$

Where ξ is the mixing parameter, $R(g_{vis})$ is the Ricci scalar corresponding to the induced metric on the visible brane. H is the electroweak Higgs boson in the five dimensional universe before rescaling. The term in Eq. (3) will present the Higgs-radion mixing in the model. The mixing of Higgs with another particle is very imperative in future collider experiments. Phenomenologically, the mixing will modify the Higgs and radion remarkably.

Particles, hardly observed in the Large Hadron Collider (LHC) experiments, are produced by weak and electromagnetic rather than strong interactions, mainly decay to τ leptons or to lighter quarks and gluons, or decay with diminutive energy release [6]. Regarding other colliders like the International Linear Collider (ILC), its strength is noticeable in that the experiments are sensitive to new particles with low probability or hard-to-detect decay schemes. Experimentally, the reaction cross sections in linear acceleration, namely ILC or e^+e^- collider, have a direct and huge dependence on the beam polarizations, physics cases of the ILC/ e^+e^- studies are emphasized in [6-9]. In the SM, relativistic left-handed and right-handed polarized electrons are totally different particles, with different electroweak quantum numbers. Hence, measurements with different beam polarization can measure distinctive reactions, which leads to direct insight into the new physics. Longitudinal polarization is maintained at linear colliders, and a polarized source of electrons or positrons can produce a comparable effect of polarization in collisions.

Two fundamental processes in modern particle physics are studied with the contribution from the standard model exchanges and unparticle exchange including both vector and scalar components. Physics of e^+e^- collisions has two prominent aspects to be mentioned in [10]. The first one, as previously mentioned, the linear collider provides longitudinally polarized electron and positron beams. The control of the beam polarization can be a powerful tool for e^+e^- physics. The ILC is expected to provide highly polarized beams with the possibility of switching the polarization orientation, which

effectively affects the number of observables [11, 12]. Another important aspect is that the center of mass energy of collisions is affected by both the initial state radiation and the beamstrahlung radiation. Both these radiations broaden the e^+e^- center of mass energy distribution and produce photons that are induced in γγ and eγ reactions. Their contribution to the additional backgrounds on account of independent low-$\sqrt{s}$ *ep* and *pp* reactions is significant since the rate of events is energy dependent. In the rest of the work, two Bhabha and Møller scatterings, under the effect of unparticles in the RS model, are concentrated.

Based on the effective field theory of low energies [13] and unusual virtual effects in high energy processes [14], H. Georgi has proposed the new physics containing a coupling between the new scale invariant sector operator (O_{BZ}) – described by Banks-Zaks (BZ) fields with the dimension d_{BZ} and the standard model one O_{SM} with dimension n at the scale of ultraviolet as follows

$$\frac{1}{M_U^{d_{SM}+d_{BZ}-4}} O_{SM} O_{BZ} \tag{4}$$

where d_{SM} and d_{BZ} are dimensions of mass of *SM* and *BZ* fields, respectively. The two sectors SM and BZ interact via the particle exchange and its mass scale is M_U. The *BZ* operators become the unparticle operators O_U below the energy Λ_U owing to dimensional transmutation from the effects of renormalization in the *BZ* sector [15], expression (4) will have the form

$$C_{O_U} \frac{\Lambda_U^{d_{BZ}-d_U}}{M_U^{d_{SM}+d_{BZ}-4}} O_{SM} O_U \tag{5}$$

where d_U is the scaling dimension of the unparticle operator O_U and the constant C_{O_U} is a coefficient function. The scalar and vector unparticle operators as propagators are focused on for the process we studied, they transform under the standard model gauge group as a standard model singlet [16, 17]. The following Feynman rules are presented in [16], which are from the effective interactions satisfying the gauge symmetry with SM fields. These Feynman rules are having the form

$$\begin{gathered} i\frac{\lambda_0}{\Lambda_U^{d_U-1}},\ \frac{-\lambda_0}{\Lambda_U^{d_U-1}}\gamma^5,\ \frac{\lambda_0}{\Lambda_U^{d_U}}p,\ 4i\frac{\lambda_0}{\Lambda_U^{d_U}}\left(-p_1.p_2 g^{\mu\nu}+p_1^{\nu}p_2^{\mu}\right) \\ i\frac{\lambda_1}{\Lambda_U^{d_U-1}}\gamma^{\mu},\ i\frac{\lambda_1}{\Lambda_U^{d_U-1}}\gamma^{\mu}\gamma^5 \end{gathered} \tag{6}$$

where λ_i are effective couplings $(C_{O_U^i}\Lambda_U^{d_{BZ}})/M_U^{d_{SM}+d_{BZ}-4}$ and dimensionless from expression (5) with the index i = 0, 1 or 2 corresponding to the scalar, vector and tensor unparticle operators, respectively.

The scalar and vector unparticle propagators have the following form

$$\begin{aligned} \Delta_{scalar}(q^2) &= \frac{A_{d_U}}{2\sin(d_U\pi)}(-q^2)^{d_U-2} \\ \Delta_{vector}(q^2)_{\mu\nu} &= \frac{A_{d_U}}{2\sin(d_U\pi)}(-q^2)^{d_U-2}\pi_{\mu\nu}(q) \end{aligned} \tag{7}$$

where

$$A_{d_U} = \frac{16\pi^2\sqrt{\pi}}{(2\pi)^{2d_U}} \frac{\Gamma(d_U + 1/2)}{\Gamma(d_U - 1)\Gamma(2d_U)}, \ \pi_{\mu\nu}(q) = -g_{\mu\nu} + \frac{q_\mu q_\nu}{q^2} \tag{8}$$

$(-q^2)$ is positive in the t- and u-channel, but negative in the s-channel process

$$(-q^2) = \begin{cases} \left|q^2\right|^{d_U-2} & q^2 < 0 \\ \left|q^2\right|^{d_U-2} e^{-id_U\pi} & q^2 > 0 \end{cases} \tag{9}$$

2. The process $e^+e^- \to e^+e^-$

Feynman diagrams of the process $e^+e^- \to e^+e^-$ is schematically described in Figure 1.

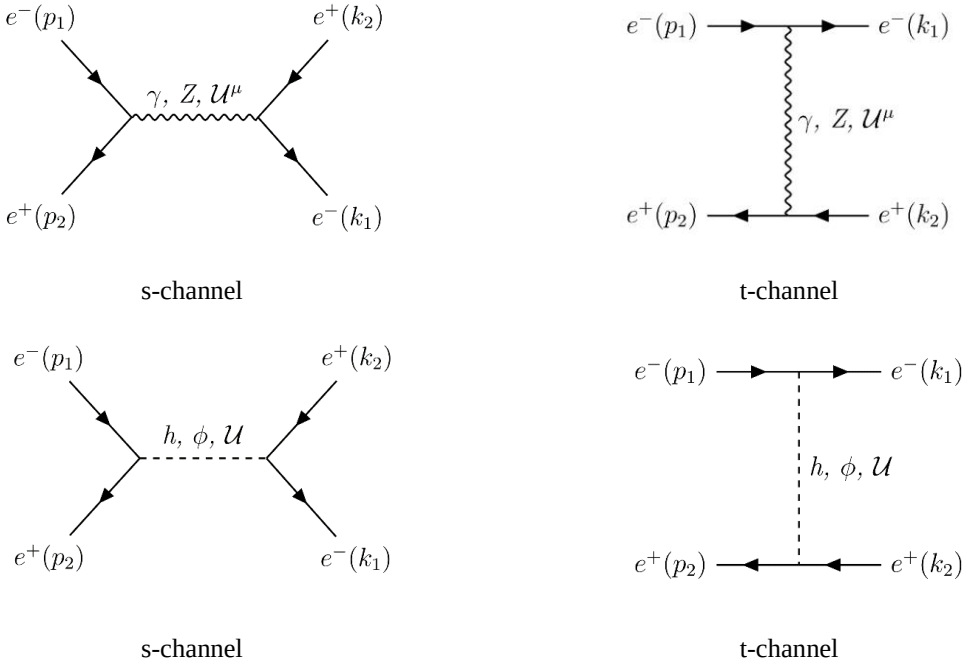

Figure 1. Feynman diagrams of the process $e^+e^- \to e^+e^-$.

In the presence of Feynman rules (6) and effective interactions, Bhabha scattering $e^+e^- \to e^+e^-$ is shown in Figure 1,where the propagating contributions are γ, Z, h, ϕ, scalar and vector unparticles U and U^μ

$$\begin{aligned} e^+ + e^- &\xrightarrow{\gamma,\, Z,\, U^\mu} e^+ + e^- & \qquad e^- + e^- &\xrightarrow{\gamma,\, Z,\, U^\mu} e^- + e^- \\ e^+ + e^- &\xrightarrow{h,\, \phi,\, U} e^+ + e^- & \qquad e^- + e^- &\xrightarrow{h,\, \phi,\, U} e^- + e^- \end{aligned} \tag{10}$$

The transition amplitudes in the s-channel and t-channel are given via (γ, Z, U^μ) exchange:

$$M_{s\gamma} = \frac{ie^2}{q_s^2}\bar{v}(p_2)\gamma_\mu u(p_1)\bar{u}(k_1)\gamma^\mu v(k_2) \tag{11}$$

$$M_{sZ} = \left(\frac{g}{4\cos\theta_W}\right)^2 \frac{i}{q_s^2 - m_Z^2}\left[g_{\mu\nu} - \frac{q_\mu q_\nu}{m_Z^2}\right]\bar{v}(p_2)\gamma^\nu[(1-4s_W^2)+\gamma_5]u(p_1) \times \bar{u}(k_1)\gamma^\mu[(1-4s_W^2)+\gamma_5]v(k_2) \tag{12}$$

$$M_{sU^\mu} = -\left(\frac{\lambda_1}{\Lambda_U^{d_U-1}}\right)^2\left(\frac{A_{d_U}\left(-q_s^2\right)^{d_U-2}}{2\sin\left(d_U\pi\right)}\right)\left[-g_{\mu\nu} + \frac{q_\mu q_\nu}{q_s^2}\right]\bar{v}(p_2)\gamma^\nu\left(1+\gamma_5\right)u(p_1) \times \bar{u}(k_1)\gamma^\mu(1+\gamma_5)v(k_2) \tag{13}$$

$$M_{t\gamma} = \frac{ie^2}{q_t^2}\bar{v}(p_2)\gamma_\mu v(k_2)\bar{u}(k_1)\gamma^\mu u(p_1) \tag{14}$$

$$M_{tZ} = \left(\frac{g}{4\cos\theta_W}\right)^2 \frac{i}{q_t^2 - m_Z^2}\left[g_{\mu\nu} - \frac{q_\mu q_\nu}{m_Z^2}\right]\bar{v}(p_2)\gamma^\nu[(1-4s_W^2)+\gamma_5]v(k_2) \times \bar{u}(k_1)\gamma^\mu[(1-4s_W^2)+\gamma_5]u(p_1) \tag{15}$$

$$M_{tU^\mu} = -\left(\frac{\lambda_1}{\Lambda_U^{d_U-1}}\right)^2\left(\frac{A_{d_U}\left(-q_t^2\right)^{d_U-2}}{2\sin\left(d_U\pi\right)}\right)\left[-g_{\mu\nu} + \frac{q_\mu q_\nu}{q_t^2}\right]\bar{v}(p_2)\gamma^\nu\left(1+\gamma_5\right)v(k_2) \times \bar{u}(k_1)\gamma^\mu(1+\gamma_5)u(p_1) \tag{16}$$

via (h, ϕ , U) exchange

$$M_{sh} = -i\left(\frac{g}{2}\left[\frac{m_e}{m_W}\left(d+\gamma b\right)\right]\right)^2 \frac{1}{q_s^2 - m_h^2}\bar{v}\left(p_2\right)u\left(p_1\right)\bar{u}\left(k_1\right)v\left(k_2\right) \tag{17}$$

$$M_{s\phi} = -i\left(\frac{g}{2}\left[\frac{m_e}{m_W}\left(c+\gamma a\right)\right]\right)^2 \frac{1}{q_s^2 - m_\phi^2}\bar{v}\left(p_2\right)u\left(p_1\right)\bar{u}\left(k_1\right)v\left(k_2\right) \tag{18}$$

$$M_{sU} = -\left(\frac{\lambda_0}{\Lambda_U^{d_U-1}}\right)^2\left(\frac{A_{d_U}\left(-q_s^2\right)^{d_U-2}}{2\sin\left(d_U\pi\right)}\right)\bar{v}\left(p_2\right)\left(1+i\gamma_5 - \frac{iq_s}{\Lambda_U}\right)u\left(p_1\right)\bar{u}\left(k_1\right)\left(1+i\gamma_5 - \frac{iq_s}{\Lambda_U}\right)v\left(k_2\right) \tag{19}$$

$$M_{th} = -i\left(\frac{g}{2}\left[\frac{m_e}{m_W}\left(d+\gamma b\right)\right]\right)^2 \frac{1}{q_t^2 - m_h^2}\bar{v}\left(p_2\right)u\left(p_1\right)\bar{u}\left(k_1\right)v\left(k_2\right) \tag{20}$$

$$M_{t\phi} = -i\left(\frac{g}{2}\left[\frac{m_e}{m_W}\left(c+\gamma a\right)\right]\right)^2 \frac{1}{q_t^2 - m_\phi^2}\bar{v}\left(p_2\right)u\left(p_1\right)\bar{u}\left(k_1\right)v\left(k_2\right) \tag{21}$$

$$M_{tU} = -\left(\frac{\lambda_0}{\Lambda_U^{d_U-1}}\right)^2\left(\frac{A_{d_U}\left(-q_t^2\right)^{d_U-2}}{2\sin\left(d_U\pi\right)}\right)\bar{v}\left(p_2\right)\left(1+i\gamma_5 - \frac{iq_t}{\Lambda_U}\right)u\left(p_1\right)\bar{u}\left(k_1\right)\left(1+i\gamma_5 - \frac{iq_t}{\Lambda_U}\right)v\left(k_2\right) \tag{22}$$

where $q_s = p_1 + p_2 = k_1 + k_2$, $q_t = k_2 - p_2 = p_1 - k_1$.

The differential cross section of the process as the expression $\frac{d\sigma}{d\cos\theta} = \frac{1}{128\pi s}\left|\frac{\vec{k_1}}{\vec{p_1}}\right|\left|M_{fi}\right|^2$ [18] is evaluated, where M_{fi} is the amplitude of transition, $s = (p_1 + p_2)^2$ and θ is the scattering angle between $\vec{p_1}$ and $\vec{k_1}$.

3. Results and Discussion

The main parameters selected are as follows: the vacuum expectation of the radion field is $\Lambda_\phi = 5$ TeV [19], the radion mass $m_\phi = 10$ GeV [20], the mass of Higgs boson $m_h = 125$ GeV, the mixing parameter $\xi = 1/6$. The following parameters of unparticle are: $\Lambda_U = 1000$ GeV, $\lambda_0 = \lambda_1 = 1$ and d_U = 1.7 which is also chosen in the range of [1.1, 1.9] for further evaluations.

In Figure 2, the plots are the correlation between the possible and frontier energy reach of the total cross-section (TCS) concerning the unparticle scaling dimension. Regarding the process, in the center-of-mass energy region from 250 GeV to 1 TeV, the TCS diminishes as d_U is up from 1.1 to 1.9, with the sharper decrease in the interval of [1.1, 1.4]. In contrast, the TCS changed to a limited extent throughout d_U's values 1.4 to 1.9. The scenario 3 TeV energy upgrade of CLIC colliders gives us that the TCS shrinks more steadily than itself in the lower energies below 3 TeV; however, the figure increase when d_U is around from 1.6 to 1.9. The dependence of TCS on the scaling dimension d_U and the center-of-mass energy is strong, feasibly leading to new physics effects in the high energy reach.

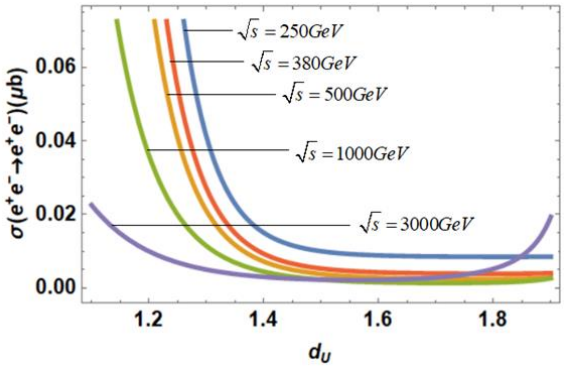

Figure 2. The total cross-sections at key level of energy versus the scaling dimension.

We investigate the cross-section versus various center-of-mass energies with three values of scaling dimension (Figure 3). In both processes, the contribution of unparticles in RS(U) is rather large. However, Higgs-radion contribution is negligible that resulting in the TCSs in SM and RS being similar in values.

In Figure 3, the TCSs of two models SM, RS become less significant in the high energies from 1.5 to 3 TeV, which might result in separate signals from different models. Considering RS(U) model in this process, the TCS increases rapidly in the high energies above 1.5 TeV as d_U equals 1.7, especially 1.9. Further, the TCS in RS(U) approximately SM, RS model that can be implied that the unparticles contribution is inconsiderable in a region of low energies below 500 GeV. We have the largest values of TCS when the scale dimension is 1.9, belonging to the high energy 2.5 – 3 TeV.

We plot the TCS in all three models when the particles are in polarized conditions: e_L^- (left-handed electron), e_R^- (right-handed electron), e_L^+ (left-handed positron), and e_R^+ (right-handed positron). The incoming and outgoing beams investigated and plotted are $e_L^-e_L^-$, $e_R^-e_R^-$, $e_L^+e_R^-$, $e_R^+e_L^-$, $e_L^+e_L^-$, $e_R^+e_R^-$; besides, the other polarized cases with their contribution are very small and hence not included in our final numerical results. For two models SM and RS without unparticles (Figure 4), the TCSs of $e_L^+e_L^-$, $e_R^+e_R^-$ beams in both processes have the equal value region because that Higgs-radion contributes insignificantly at 10^{-24} μb. As opposed to the pure left- or right-handed particle beams, the mixed conditions of polarization only have a small contribution to the TCS in the RS model.

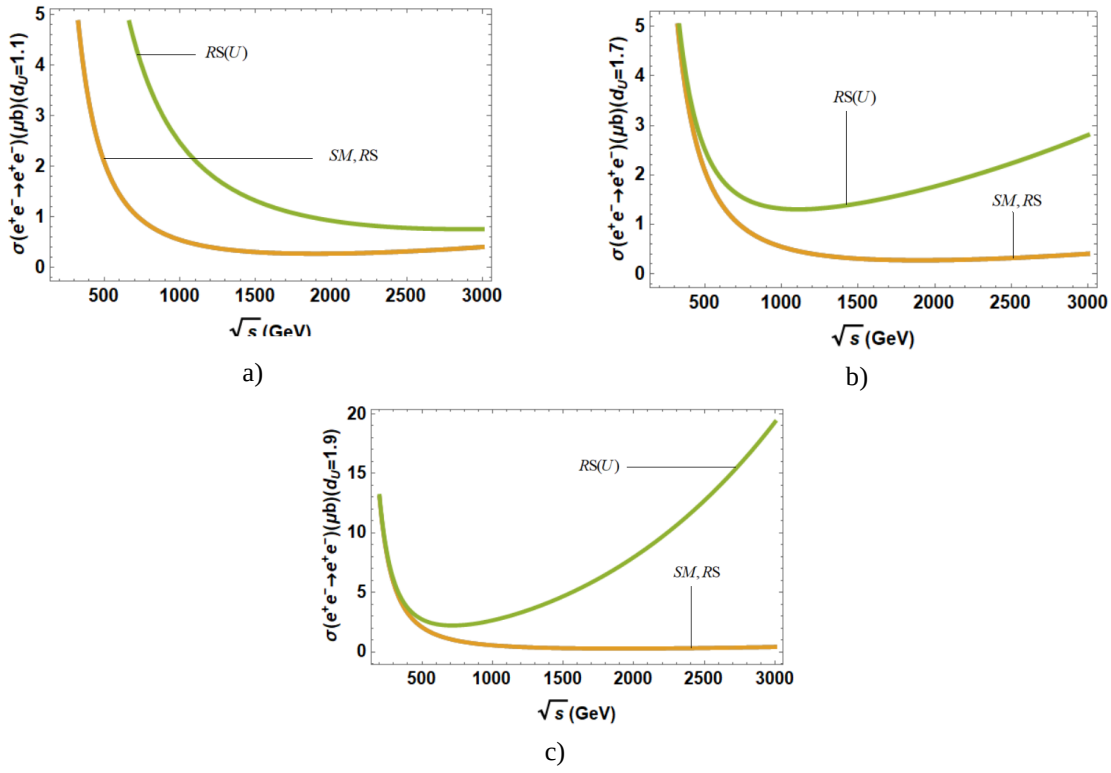

Figure 3. The total cross-sections of $e^+e^- \to e^+e^-$ in SM, RS, and RS(U) models with the chosen scaling dimension 1.7.

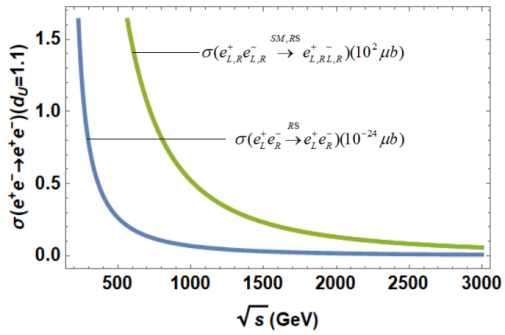

Figure 4. The polarized total cross sections versus the center-of-mass energy in SM and RS models.

In the next part, we plot the TCS in RS(U) model versus the center-of-mass energies including the multi-TeV region. The scale dimensions are chosen as 1.1, 1.7, and 1.9, which shows us a more direct comparison of unparticle effects. When the scaling dimension 1.1, in the low energies around 0 and 1 TeV for both processes, the TCSs of every polarized beam all go down promptly and become flat in the high energy region (Figure 5a).

For the d_U = 1.7 (Figure 5b), the TCSs of the polarized $e_L^+e_R^-$, beams in RS(U) gradually go up throughout the energy region from 0 to 3 TeV. The TCS of the polarized $e_L^+e_L^-$, $e_R^+e_R^-$, beams make up for the contribution in the low energies below 1 TeV, much larger than the TCS of the $e_L^+e_R^-$ beams.

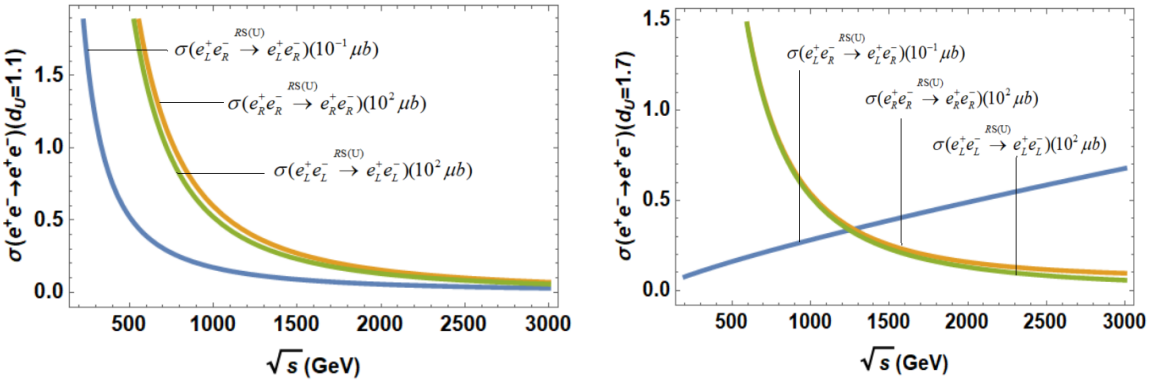

(a) (b)

Figure 5. The total cross-sections of $e^+e^- \to e^+e^-$ in RS(U) model with the chosen scaling dimension are 1.7.

This time we plot the TCS for the polarization cases of the particle beams concerning the scaling dimension 1.9 (Figure 6). In the low energy region below 500 GeV, the TCS of the polarized $e_L^+e_L^-$, $e_R^+e_R^-$beams contribute largely to both processes. While the mixed conditions $e_L^+e_R^-$, we see the rise of the TCS when the energies rise.

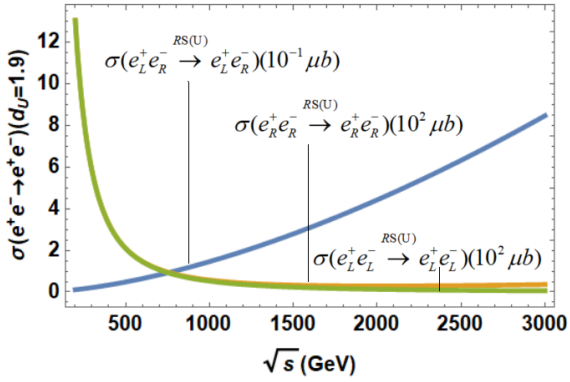

Figure 6. The polarized total cross sections versus the center-of-mass energy in RS(U) model.

To sum up the process, the calculated number of events in one year for the process is shown in Table 1 in the following models: SM, RS, and RS(U). The energy reaches selected for the processes are based on the current development and the proposed luminosity and energy upgrade scenarios including ILC (International Linear Collider), and Compact Linear Collider (CLIC) [9, 21-24].

Table 1 shows that the number of events for two models SM and RS is equivalent, meanwhile the figure for RS(U) with the contribution of unparticles is more considerable than the other models. Additionally, the rise of scaling dimension d_U that leads to a notable increase in the ratio of event numbers between models, especially in the higher energy 1 TeV ILC and 3 TeV CLIC. The ratio of event numbers between RS(U) and SM and RS will escalate as the scaling dimension reaches 1.9 in the region of frontier energy 3 TeV which becomes more physically important in exploring the realms of new physics.

Table 1. The events number for the $e^+e^- \rightarrow e^+e^-$ in SM, RS model, and RS(U) model.

Colliders	International Linear Collider (ILC)			The Compact Linear Collider (CLIC)	
ECM (GeV)	250	500	600	380	3000
Luminosity (10^{34})	1.35	1.8	4.9	1.5	6
N_{SM}	1.12×10^9	3.74×10^8	2.68×10^8	5.38×10^8	2.44×10^8
N_{RS}	1.12×10^9	3.74×10^8	2.68×10^8	5.38×10^8	2.44×10^8
$d_U = 1.1$					
$N_{RS(U)}$	3.48×10^9	1.41×10^9	3.85×10^9	1.88×10^9	4.56×10^9
$N_{RS(U)}/N_{SM}$	3.108	3.782	4.505	3.493	1.873
$d_U = 1.7$					
$N_{RS(U)}$	1.15×10^9	4.51×10^8	6.46×10^8	5.9×10^8	1.68×10^9
$N_{RS(U)}/N_{SM}$	1.029	1.207	2.409	1.096	6.903
$d_U = 1.9$					
$N_{RS(U)}$	1.15×10^9	4.92×10^8	1.3×10^9	6.01×10^8	3.74×10^8
$N_{RS(U)}/N_{SM}$	1.026	1.316	4.831	1.117	47.58

4. Conclusion

In summary, the total cross-sections versus the scaling dimension d_U and the center-of-mass energy $\sqrt{s}$ is evaluated with the appropriate parameters and energy reaches that have been concerned recently. The numerical results and the plots show that the total cross-sections of the process in RS(U) have more considerable increases when compared to the two models SM and RS, without unparticles. The contribution of Higgs and Radion to the processes is minimal, which induces the figure equivalence of the cross-sections of SM and RS. When we have the polarized cases of the incoming and outgoing beams of particles, the TCSs of the polarized left-handed conditions or right-handed conditions of particle beams are larger than mixed conditions between left- and right-handed and any other polarized. With the emergence of unparticles, the total cross-section of the process $e^+e^- \rightarrow e^+e^-$ at near and multi-TeV energies is much greater than itself at lower energy reach below roughly 3 TeV when the unparticle dimension of scale d_U is 1.7 and 1.9.

References

[1] L. Randall, R. Sundrum, A Large Mass Hierarchy from a Small Extra Dimension, Phys. Rev. Lett. Vol. 83, No. 17, 1999, pp. 3370-3373, https://link.aps.org/doi/10.1103/PhysRevLett.83.3370.

[2] N. A. Hamed, S. Dimopoulos, G. Dvali, The Hierarchy Problem and New Dimensions at a Millimeter, Phys. Lett. B, Vol. 429, No. 3, 1998, pp. 263-272, arXiv:hep-ph/9803315v1.

[3] W. D. Goldberger, M. B. Wise, Modulus Stabilization with Bulk Fields, Phys. Rev. Lett. Vol. 83, No. 24, 1999, pp. 4922-4925; W. D. Goldberger, M. B. Wise, Bulk fields in the Randall-Sundrum Compactification Scenario, Phys. Rev. D Vol. 60, No. 10, 1999, pp. 107505, https//doi.org/10.1103/PhysRevD.60.107505.

[4] M. Luty, R. Sundrum, Radius Stabilization and Anomaly-Mediated Supersymmetry Breaking, Phys. Rev. D, Vol. 62, No. 3, 2000, pp. 035008, https//doi.org/10.1103/physrevd.62.035008.

[5] C. Csaki, M. Graesser, L. Randall, J. Terning, Cosmology of Brane Models with Radion Stabilization, Phys. Rev. D, Vol. 62, No. 3, 2000, pp. 045015, https//doi.org/10.1103/physrevd.62.045015.

[6] K. Fujii, C. Grojean, M. E. Peskin, T. Barklow, Y. Gao, S. Kanemura, H. Kim, J. List, M. Nojiri, M. Perelstein, R. Pöschl, J. Reuter, F. Simon, T. Tanabe, J. D. Wells, J. Yu, H. Baer, M. Berggren, S. Heinemeyer, S. L. Lehtinen, J. Tian, G. Wilson, J. Yan, H. Murayama, J. Brau, Physics Case for the 250 GeV Stage of the International Linear Collider, 2018, https//doi.org/10.48550/ARXIV.1702.05333.

[7] H. Baer, M. Berggren, J. List, M. M. Nojiri, M. Perelstein, A. Pierce, W. Porod, T. Tanabe, Physics Case for the ILC Project: Perspective from Beyond The Standard Model, ePrint 1710.07621, 2013 https//doi.org/10.48550/ARXIV.1307.5248.

[8] A. Aryshev, T. Behnke et al., The International Linear Collider: Report to Snowmass 2021, 2022, eprint 2203.07622, https//doi.org/10.48550/ARXIV.2203.07622.

[9] T. Lesiak, Future e^+e^- Colliders at the Energy Frontier, EPJ Web Conf, Vol. 206, 2019, pp. 08001, https//doi.org/10.1051/epjconf/201920608001.

[10] K. Fujii, C. Grojean, M. E. Peskin, T. Barklow, Y. Gao, S. Kanemura, J. List, M. Nojiri, M. Perelstein, R. Poeschl et al., ILC Study Questions for Snowmass 2021, ePrint 2007.03650, arXiv:2007.03650v3.

[11] K. Fujii, C. Grojean, M. E. Peskin, T. Barklow, Y. Gao, S. Kanemura, H. Kim, J. List, M. Nojiri, M. Perelstein et al., Tests of the Standard Model at the International Linear Collider, 2019, ePrint 1908.11299, arXiv:1908.11299v4.

[12] K. Fujii, C. Grojean, M. E. Peskin, T. Barklow, Y. Gao, S. Kanemura, H. Kim, J. List, M. Nojiri, M. Perelstein et al., The Role of Positron Polarization for the Initial 250 GeV Stage of the International Linear Collider, Vol 460, 2008, pp. 131-243, arXiv:hep-ph/0507011v1.

[13] T. Banks, A. Zaks, On the Phase Structure of Vector-like Gauge Theories With Massless Fermions, Nucl. Phys. B, Vol. 196, No. 2, 1982, pp. 189-204.

[14] H. Georgi, Unparticle Physics, Phys. Rev. Lett. Vol. 98, No. 22, 2007, pp. 221601, https//doi.org/10.1103/physrevlett.98.221601.

[15] S. Coleman, E. Weinberg, Radiative Corrections as the Origin of Spontaneous Symmetry Breaking, Phys. Rev. D Vol 7, No. 6, 1973, pp. 1888-1910, 10.1103/PhysRevD.7.1888.

[16] K. Cheung, W. Y. Keung, T. C. Yuan, Collider Phenomenology of Unparticle Physics, Phys. Rev. D Vol. 76, No. 5, 2007, pp. 055003, https//doi.org/10.1103/PhysRevD.76.055003.

[17] S. L. Chen, X. G. He, Interactions of Unparticles with Standard Model Particles, Phys. Rev. D Vol. 76, No. 9, 2007, pp. 091702, https//doi.org/10.1103/PhysRevD.76.091702.

[18] M. E. Peskin, D. V. Schroeder, An Introduction to Quantum Field Theory, Addision-Wesley Publishing, 2018.

[19] D. Dominici, B. Grzadkowski, J. F. Gunion, M. Toharia, The Scalar Sector of the Randall–Sundrum Model, Nucl. Phys. B, Vol. 671, 2003, pp. 243-292, https://doi.org/10.1016/j.nuclphysb.2003.08.020.

[20] D. V. Soa, D. T. L. Thuy, N. H. Thao, T. D. Tham, Radion Production γe^- Collisions, Mod. Phys. Lett. A, Vol. 27, No. 23, 2012, https://doi.org/10.1142/S021773231250126X.

[21] P. Bambade, T. Barklow, T. Behnke et al., The International Linear Collider: A Global Project, ePrint 1903.01629, 2019, arXiv:1903.01629v3.

[22] M. Harrison, M. Ross, N. Walker, Luminosity Upgrades For ILC, ePrint 1308.3726, 2013, arXiv:1308.3726v1.

[23] D. Dannheim, P. Lebrun, L. Linssen, D. Schulte, F. Simon, S. Stapnes, N. Toge, H. Weerts, J. Wells, CLIC e^+e^- Linear Collider Studies Process 2013, ePrint 1305.5766, 2013, arXiv:1305.5766v1.

[24] L. Linssen, A. Miyamoto, M. Stanitzki, H. Weerts, Physics and Detectors At CLIC: CLIC Conceptual Design Report, ePrint 1202.5940, 2012, arXiv:1202.5940v1.